

# BULK NANOSTRUCTURED SHAPE MEMORY ALLOYS

THOMAS WAITZ

Physics of Nanostructured Materials, Faculty of Physics, University of Vienna,  
Boltzmannngasse 5, 1090 Vienna, Austria.  
thomas.waitz@univie.ac.at

**ABSTRACT:** This paper starts with a brief introduction to bulk nanostructured materials. Bulk nanocrystalline materials processed by methods of severe plastic deformation show mechanical properties and phase structures that can differ significantly from those of their coarse grained counterparts. In the case of NiTi shape memory alloys, a nanocrystalline structure is obtained via the devitrification of an intermediate amorphous phase induced by high pressure torsion. Grain sizes in the range of 5 to 350 nm are achieved that are free of strains and of crystal defects. The small grain size significantly impacts the martensitic phase transformation that causes unique thermomechanical properties such as the shape memory effect and superelasticity. Experimental results on the enhanced mechanical properties of nanocrystalline and ultrafine grained NiTi shape memory alloys are shortly reviewed.

**Keywords:** Nanostructures, Severe plastic deformation, Shape memory alloys, Martensite, Size effect

**RESUMO:** É feita inicialmente uma breve introdução aos materiais nanoestruturados. Materiais nanocristalinos processados impondo grandes deformações plásticas revelam propriedades mecânicas e estruturas de fase que podem diferir significativamente dos materiais de grão grosseiro. No caso de ligas de memória de forma NiTi, uma estrutura nanocristalina pode ser obtida por devitrificação de uma fase intermédia amorfa induzida por torsão e alta pressão. Tamanhos de grão da ordem dos 5 aos 350 nm são obtidos livres de deformação e de defeitos cristalinos. O tamanho de grão pequeno tem impacto significativo sobre a transformação da fase martensite, causando propriedades termomecânicas únicas, tais como efeito de memória de forma e superplasticidade. São concisamente descritos resultados experimentais relativos à melhoria das propriedades mecânicas de ligas de memória de forma nanocristalinas e de grão ultrafino NiTi

**Palavras chave:** nanoestruturas; deformação plástica severa, ligas de memória de forma, martensite, efeito de tamanho

## 1. INTRODUCTION

During the past two decades, materials with grain sizes in the range of a few nanometers to several hundreds of nanometers have stimulated numerous research activities to elucidate the fundamental physical reasons for their novel and enhanced properties [1-5]. Polycrystalline materials are denoted nanocrystalline when their average grain size and range of grain sizes are less than 100 nm. Similar, nanostructured materials are those characterized by one or several dimensions that, on the average, are less than 100 nm. Whereas, materials with grain sizes in the range of 0.1 to 1  $\mu\text{m}$  and with grain sizes larger than 1  $\mu\text{m}$  are often termed ultrafine grained and microcrystalline, respectively. To obtain nanocrystalline or nanostructured materials, two major routes of processing can be applied [6]. In the case of a bottom up approach, the materials is made up from elementary building blocks e.g. atom by atom or atomic layer by atomic layer. In the case of a top down approach, the initial microstructure is broken up e.g. by severe plastic deformation that causes grain fragmentation and significant grain refinement.

With respect to both engineering applications and scientific studies of the mechanical properties, bulk nanocrystalline materials that are free from porosity and nanovoids and with

a low amount of impurities are often desired. A very promising processing route includes methods of severe plastic deformation to yield rather large samples that are full dense and can be obtained from high purity materials [6,7]. Full dense and pure bulk nanostructured materials can also be achieved via an intermediate amorphous phase by devitrification occurring by nanocrystallization [8]. It is the aim of the present work, to give a short overview on the mechanical properties and the phase structures of nanocrystalline materials. Methods of severe plastic deformation are outlined and applied to achieve nanostructured NiTi shape memory alloys. The impact of the grain size on the martensitic phase transformation and on the morphology of the martensite in the nanograins is discussed. Finally, results presented in the literature on the mechanical properties of nanocrystalline and ultrafine grained NiTi shape memory alloys are shortly reviewed.

### 1.1 Nanocrystalline materials: Mechanical properties

In nanocrystalline materials, the physical mechanisms of plasticity including both dislocation motion within the grains and grain boundary based processes such as grain boundary sliding are topics of intense current research [5,9]. In nanograins, dislocation glide can involve partial dislocations

instead of full dislocations when the grain size is smaller than a certain threshold value [10]. Twinning was reported to occur at a nanoscale even in materials with relative high stacking fault energies. Heterogeneous plastic flow is frequently observed in nanocrystalline materials [11] and the formation and propagation of shear bands is not fully understood yet. The unique mechanisms of plasticity of nanocrystalline materials can lead to enhanced mechanical properties. As expected from the Hall-Petch relationship, mechanical strength increases with decreasing grain size and materials with exceptional large yield strengths can be achieved when their grain size is in the range of a few tens of nanometres (it should be noted that below about 100 nm, deviations of the Hall-Petch behaviour as observed in the microcrystalline state might arise; even softening might occur when the grain sizes further decreases below about 10 nm [5,11,12]).

As compared to their coarse grained counterparts, nanocrystalline materials show a variety of outstanding mechanical properties [5,9]. It is important to note that bulk nanocrystalline materials processed by severe plastic deformation lead to ultrahigh strength while maintaining good ductility [13]. Forming of nanocrystalline materials can be achieved by mechanisms of superplasticity even at rather low temperatures and/or large strain rates [14]. Wear resistance of nanocrystalline materials can be greatly enhanced. In nanocrystalline materials, mechanisms of fracture can differ from those of coarse grained materials and significantly impact fracture strength, toughness and fatigue properties [5]. Whereas some studies on fracture mechanisms and fatigue of ultrafine grained materials were carried out, in the case of nanocrystalline materials only a few investigations are available up till now.

### 1.2 Nanocrystalline materials: Phase structures and shape memory alloys

In nanocrystalline materials, the high density of grain boundaries can significantly impact the phase stability. Unique phase structures of nanocrystalline alloys and intermetallic compounds arise when they are processed by severe plastic deformation. Striking examples of new phase structures include disordering [15] and even amorphization [16-18], the dissolution of second phase particles and the enhanced solubility of otherwise immiscible elements [19].

Shape memory alloys show a martensitic phase transformation that yields unique thermomechanical properties such as the shape memory effect and superelasticity. A martensitic phase transformation is a first order solid to solid phase transformation that proceeds by co-operative movements of the atoms [20]. The martensitic phase transformation occurs upon cooling or straining from the austenitic high temperature phase to the martensite. Minimizing lattice distortions, a sequence of twin related martensitic variants can facilitate the formation of an invariant habit plane between the martensite and the parent austenite lattice. In coarse grained materials, the twinning periodicity is typically in the range of several 10 to several 100 nanometres. On a larger scale, self-accommodated arrangements can occur made up by groups of different twinned variants of the martensite. The morphology of the martensite is of crucial importance for the unique macroscopic thermo-mechanical behaviour of shape

memory materials. In the case of nanocrystalline materials, crystal size can be considerably smaller than the twinning periodicity of the martensite that forms in their coarse grained counterparts. Therefore, size effects are expected to occur that can impact the phase stability and the martensitic morphology in nanostructured materials.

### 1.3 Severe plastic deformation

Methods of severe plastic deformation (SPD) can be used to obtain bulk nanocrystalline materials that mainly form high angle grain boundaries upon the considerable refinement of the microstructure. From a scientific point of view, the most common methods of SPD are high pressure torsion (HPT) and equal channel angular pressing (ECAP) [7]. In these cases, bulk samples are subjected to a large plastic deformation at relatively low homologous temperatures. Imposing a large pressure caused by geometrical constraints of the straining devices (dies and anvils) hinders the growth of cracks and, therefore, mechanical failure.

In the case of HPT, a specimen is put between two anvils that are loaded until a high quasi-hydrostatic pressure (several GPa) builds up (specimens of a diameter of about 5 to 20 mm and an initial thickness of about 0.3 to 0.8 mm are used; cf. Fig. 1a). When the anvils are rotated with respect to each other, a shear strain is applied. The shear strain depends on the number of rotations, and specimens thickness as well as on the radial distance from the centre of the specimen. Strains obtained near the periphery of the specimen can readily exceed 100.000%. It should be noted that even rather brittle materials can be subjected to HPT. In this case, the critical step is the initial loading of the anvils until the hydrostatic pressure has build up. During loading, brittle fracture that might occur at the grain boundaries can be avoided using single crystals as starting materials [21]. In the case of ECAP, a billet is pressed through a die that contains two channels of equal diameter that have an angle of intersection of about 90° (cf. Fig. 1b). Since the cross section of the sample is not changed, the pressing can be repeated. Different routes of the deformation can be applied when the sample is rotated between repeated steps of ECAP. Depending on the number of passes, a total strain of about 1000% can be achieved.

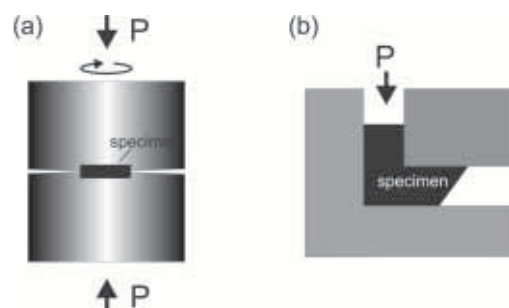


**Fig. 1.** Methods of severe plastic deformation. (a) High pressure torsion. A disc shaped specimen (typically about 10 mm diameter and 0.5 mm thickness) held between two anvils is strained in torsion under a high hydrostatic pressure (several GPa). (b) Equal channel angular pressing. A billet shaped specimen (typically about 10 mm diameter and 100 mm length) is pressed through a die made up by two channels of equal diameter that have an angle of intersection of about 90°.

## 2. NANOSTRUCTURED NiTi SHAPE MEMORY ALLOYS

Among various shape memory alloys, NiTi is most widely used for practical applications. In NiTi shape memory alloys, a martensitic phase transformation occurs from the ordered cubic B2 austenite to the monoclinic B19' martensite. Recently, nanocrystalline and ultrafine grained NiTi alloys with enhanced shape memory properties attracted considerable interest as high-tech materials [22,23].

### 2.1 HPT induced amorphization of NiTi

In NiTi shape memory alloys, severe plastic deformation by HPT [16-18,24,25] and even by cold rolling [26] can cause localized deformation by shear bands that destroys the crystalline lattice leading to a crystalline to amorphous phase transformation. The refinement of the microstructure is caused by dislocation accumulation and strain induced twinning of the martensite; a shear strain instability leads to large localized plastic deformation and to the formation of intersecting bands of nanocrystalline and amorphous phase.

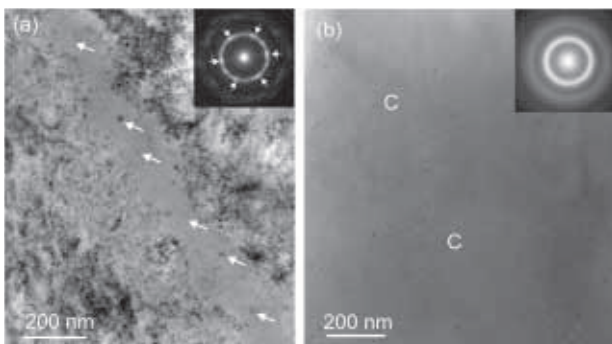


**Fig. 2.** NiTi deformed by HPT. (a) TEM bright-field image of the severely strained crystalline structure containing an amorphous shear band (strain < 1000%). Selected area electron diffraction (cf. the inset) yields a ring pattern composed of diffraction spots corresponding to a nanocrystalline phase of both B2 and B19'. Caused by a texture, six-fold intensity variations occur (indicated by arrows). The contrast of the amorphous band is rather uniform and diffuse. Retained nanocrystals are marked by arrows. (b) TEM bright-field image of the amorphous phase (strain ~ 100.000%). The diffraction pattern shows diffuse rings caused by the amorphous structure. Clusters of nanocrystals (marked by C) that have survived the severe plastic deformation are frequently observed embedded in the amorphous matrix.

Since the amorphization occurs on a nanoscale, transmission electron microscopy (TEM) was used to analyse the heterogeneous microstructure. Figure 2a shows a TEM bright-field image of a specimen taken near the centre of the HPT disc where the strain is relatively low (< 1000%). Selected area (SA) diffraction taken from the crystalline areas yields ring patterns that are caused by the strong grain refinement and by large lattice strains (cf. the inset in Fig. 2a). The diffraction pattern comprises both reflections from the B2 austenite and the B19' martensite; a six-fold intensity variation is caused by a crystallographic texture. In the TEM bright-field images, the amorphous bands that have a width

of about 100 nm show up by a uniform and rather diffuse contrast. Nanocrystals are embedded in the amorphous bands and most of them have a size of less than 30 nm. With increasing strain, HPT facilitates both strong crystal refinement and the continuous accumulation of amorphous shear bands. The crystalline volume fraction gradually decreases until only isolated nanocrystals are left embedded heterogeneously in an amorphous matrix. Finally, caused by the plastic deformation of the amorphous matrix the retained nanocrystals dissolve in the amorphous phase; when the strain exceeds about 100.000% only a few nanocrystals < 15 nm survive the HPT (cf. Fig. 2b).

### 2.2 Nanocrystallization of HPT NiTi

Upon annealing of the amorphous NiTi shape memory alloys processed by HPT, devitrification occurs by nanocrystallization. To study the mechanisms of the nanocrystallization, in-situ TEM heating experiments were carried out [27]. The devitrification occurs heterogeneously. Upon annealing, crystallites that have survived the HPT start to grow. Crystallites also nucleate predominantly near clusters of pre-existing nanocrystals that have survived the severe plastic deformation. As shown by the in-situ heating experiments, the nanocrystals grow spherically at a constant rate until they impinge upon each other.

TEM SA diffraction methods applied during the in-situ heating yield the result that the devitrification occurs by the formation of nanocrystals that have the ordered B2 high temperature phase of NiTi. The devitrification is polymorphous since no apparent change of the chemical composition upon crystallization was encountered using energy dispersive X-ray analysis [28]. Depending on both the total strain applied by the HPT deformation and the temperature of the annealing, grain sizes in the range of 5 to 350 nm were obtained after complete devitrification [18]. Most of the grains are free of dislocations and only little lattice strains were observed (cf. Fig. 3). Upon partial devitrification, nanostructured NiTi alloys are obtained containing nanocrystals embedded in an amorphous matrix [28].

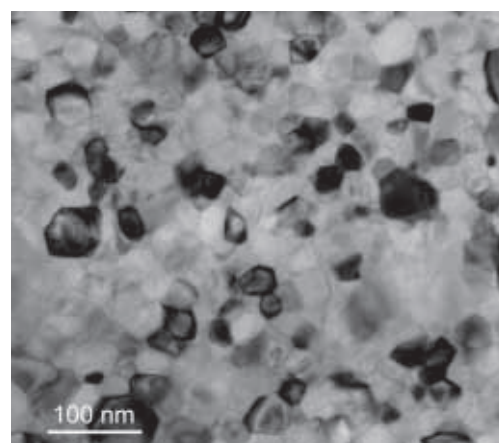


**Fig. 3.** HPT NiTi. Nanocrystalline structure obtained after complete devitrification of an intermediate amorphous phase. Most of the grains (mean size of about 60 nm) are free of dislocations and show little lattice strains only.



### 2.3 The martensitic phase transformation in nanostructured NiTi

Nanocrystalline alloys were used to study the impact of the grain size on the martensitic phase transformation. Using differential scanning calorimetry, a strong decrease of the temperature of the transformation from B2 to B19' is observed when the grain size decreases below about 100 nm. TEM experiments show that the volume fraction of the grains transformed to martensite decreases with decreasing grain size. In grains with a size smaller than about 50 nm, the transformation is even completely suppressed. To explain the effect of the grain size on the suppression of the transformation to martensite, a physical model of a transformation barrier is proposed [29]. Comprising elastic strain energy and twin boundary energy, the energy barrier increases with decreasing grain size in agreement with the suppression of the martensitic phase transformations in the nanograins.

A unique morphology of (001) compound twinned martensite is observed in the nanograins (cf. Fig. 4). Atomic scale twinning of B19' martensite is facilitated by a low specific twin boundary energy of the compound twins [30]. The formation of an ultrahigh density of twins is a prerequisite of the transformation in the nanograins to compensate the high transformation strains of B19' [29]. It should be noted that the (001) compound twins violate the well-established theory of the martensitic transformation based on the formation of invariant martensite/austenite interfaces.

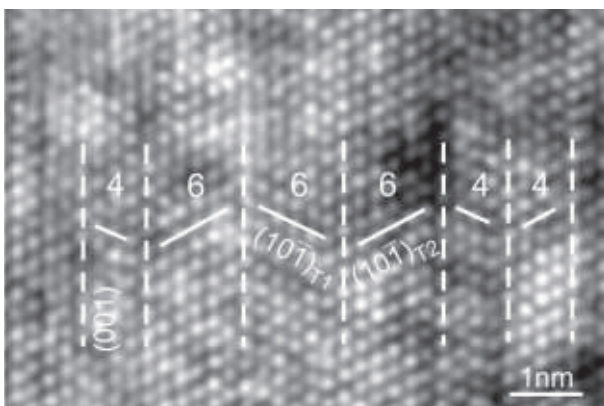


**Fig. 4.** Nanocrystalline NiTi. Atomic structure of the martensite. Experimental HRTEM image of (001) compound twins. (10 $\bar{1}$ ) lattice planes of the twins and the twin boundaries are marked by full and dashed lines mark, respectively. The numbers denote the thickness of the twins in units of (002) lattice planes.

Most of the martensitic nanograins that have a size of less than about 200 nm contain (001) compound twins. Two different morphologies of the twinned martensite are observed. A single variant of compound twinned martensite occurs below a critical grain size of about 100 nm (cf. Fig. 5a). In larger grains, a herringbone morphology of two different twinned variants of the martensite is observed (cf. Fig. 5b). In this case, additional interfaces arise between the variants V1 and V2 that are indicated by dashed lines. It is concluded that the competing transformation mechanisms

are caused by the different scaling behaviour of strain and interface energy that oppose the transformation. Minimizing the strain energy and the total interfacial energy, a single twinned variant of B19' is preferred in grains smaller than a critical size of about 100 nm. Whereas, a self-accommodated morphology composed of two twinned variants occurs in larger grains [31]. In the latter case, the energy caused by homogeneous transformation strains (proportional to the volume of the grains) is released at the expense of highly localized strains arising at additional interfaces.

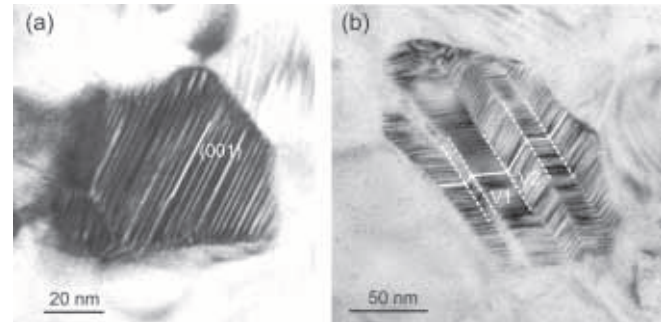


**Fig. 5.** Martensitic nanograins of NiTi. TEM bright field images of ultrafine twins (running parallel to the full lines). (a) Single variant of twinned martensite. (b) Herringbone morphology of two variants V1 and V2 of twinned martensite (dashed lines indicate the junction planes of V1 and V2).

### 2.4 Mechanical properties of nanocrystalline NiTi

In the literature, several investigations of the mechanical properties of nanocrystalline and ultrafine grained NiTi shape memory alloys were carried out [32-35]. To achieve a homogenous and stable structure and to tailor the mechanical properties, NiTi alloys of different compositions were subjected to HPT and ECAP including multiple steps of severe plastic deformation followed by cold rolling and annealing. Optimised structures were obtained that lead to ultrahigh strength and good ductility in combination with enhanced functional properties of the shape memory effect and superelasticity. Nanocrystalline NiTi shape memory alloys show high recovery stresses and a shape recovery of up to 10%. In ultrafine grained NiTi alloys, the superelastic effect is improved since the cyclic reversibility is greatly enhanced. It should be noted that systematic investigations of the fatigue behaviour and of the fracture mechanisms of nanocrystalline and ultrafine grained NiTi shape memory alloys are not available in the literature thus offering opportunities of future research in that field.

## 3. SUMMARY

Using methods of severe plastic deformation, full dense bulk nanocrystalline and ultrafine grained materials that are free from impurities can be processed. Bulk nanocrystalline metals and alloys show outstanding mechanical properties such as ultrahigh strength in combination with good ductility. The phase stability of alloys and intermetallic compounds processed by severe plastic deformation can

differ significantly from that of their coarse grained counterparts. Using HPT, nanostructured NiTi shape memory alloys can be obtained via the devitrification of an intermediate amorphous structure. In nanocrystalline NiTi, a unique morphology of the martensite occurs that is caused by the minimization of the strain and interface energy opposing the martensitic transformation. When NiTi is subjected to severe plastic deformation, ultrahigh strength and good ductility is achieved in combination with enhanced functional properties of the shape memory effect and superelasticity. With respect to fracture and fatigue, nanocrystalline materials processed by severe plastic deformation open up a field that is rich in opportunities for future research.

## ACKNOWLEDGEMENTS

T. Waitz acknowledges the support by the research project "Bulk Nanostructured Materials" within the research focus "Materials Science" of the University of Vienna. The author also thanks Professor R.Z. Valiev and Dr. V. Kazykhanov for the HPT deformation of NiTi samples.

## REFERENCES

- [1] S. X. McFadden, R. S. Mishra, R. Z. Valiev, A. P. Zhilyaev and A. K. Mukherjee, *Nature* **398** (1999) 684.
- [2] Y. M. Wang, M. Chen, F. Zhou and E. Ma, *Nature* **419** (2002) 912.
- [3] C. C. Koch, *Scripta Mater.* **49** (2003) 657.
- [4] H. Gleiter, *Acta Mater.* **48** (2000) 1.
- [5] K. S. Kumar, H. Van Swygenhoven and S. Suresh, *Acta Mater.* **51** (2003) 5743.
- [6] C. C. Koch, *J. Mater. Sci.* **42** (2007) 1403-1414.
- [7] R. Z. Valiev, R. K. Islamgaliev and I. V. Alexandrov, *Progr. Mater. Sci.* **45** (2000) 103.
- [8] G. Wilde, N. Boucharat, R. Hebert, H. Rösner and R. Z. Valiev, *Mater. Sci. Eng. A* **449-451** (2007) 825.
- [9] M. Dao, L. Lu, R. J. Asaro, J. T. M. De Hosson and E. Ma, *Acta Mater.* **55** (2007) 4041.
- [10] M. Chen, E. Ma, K. J. Hemker, H. Sheng, Y. Wang and X. Cheng, *Science* **300** (2003) 1275.
- [11] J. R. Trelewicz and C. A. Schuh, *Acta Mater.* **55** (2007) 5948.
- [12] J. Schiøtz and K. W. Jacobsen, *Science* **301** (2003) 1357.
- [13] R. Z. Valiev, *Adv. Eng. Mater.* **5** (2003) 296.
- [14] V. Yamakov, D. Wolf., S. R. Phillpot, A. K. Mukherjee and H. Gleiter, *Nature Mater.* **3** (2004) 43.
- [15] C. Rentenberger and H. P. Karnthaler, *Acta Mater.* **53** (2005) 3031.
- [16] J. Y. Huang, Y. T. Zhu, X. Z. Liao and R. Z. Valiev, *Phil. Mag. Lett.* **84** (2004) 183.
- [17] A. V. Sergueeva, C. Song, R. Z. Valiev and A. K. Mukherjee, *Mater. Sci. Eng. A* **339** (2003) 159.
- [18] T. Waitz, V. Kazykhanov and H. P. Karnthaler, *Acta Mater.* **52** (2004) 137-147.
- [19] X. Sauvage and R. Pippan, *Mater. Sci. Eng. A* **410-411** (2005) 345.
- [20] G. B. Olson, Martensite (G. B. Olson and W. S. Cohen, Eds.) AMS International (1992) p. 1.
- [21] C. Mangler, C. Rentenberger, I. Humer, L. Reichhart and H. P. Karnthaler, *Micr. Microanal.* **13-S03** (2007) 298.
- [22] R. Z. Valiev, *Nature Mater.* **3** (2004) 511.
- [23] I. Karaman., A. V. Kulkarni and Z. P. Luo, *Philos. Mag A* **85** (2005) 1729.
- [24] C. Rentenberger, T. Waitz and H. P. Karnthaler, *Mater. Sci. Eng. A* **462** (2007) 283.
- [25] H. P. Karnthaler, T. Waitz, C. Rentenberger and B. Mingler, *Mater. Sci. Eng. A* **387-389** (2004) 777.
- [26] J. Koike, D. M. Parkin and M. Nastasi., *J. Mater. Res.* **5** (1990) 1414.
- [27] M. Peterlechner, T. Waitz, I. Moder and H. P. Karnthaler, *Micro. Microanal.* **13-S03** (2007) 302.
- [28] T. Waitz and H. P. Karnthaler, *Acta Mater.* **52** (2004) 5461.
- [29] T. Waitz, T. Antretter, F. D. Fischer, N. K. Simha and H. P. Karnthaler, *J. Mech. Phys. Sol.* **55** (2007) 419.
- [30] T. Waitz, D. Spisak, J. Hafner and H. P. Karnthaler, *Europhys. Lett.*, **71** (2005) 98.
- [31] T. Waitz, W. Pranger, T. Antretter and F. D. Fischer, *Mater. Sci. Eng. A* **481-482** (2008) 479.
- [32] V. G. Pushin, V. V. Stolyarov, R. Z. Valiev, T. C. Lowe and Y. T. Zhu, *Mater. Sci. Eng. A* **410-41** (2005) 386.
- [33] B. Kockar, I. Karaman, J. I. Kim and Y. Chumlyakov, *Scripta Mater.* **54** (2006) 2203.
- [34] S. D. Prokoshkin et al., *Metal Sci. Heat Treat.* **47** (2005) 182.
- [35] V. G. Pushin et al., *Mater. Trans.* **503-504** (2006) 539.